processes

MDPI

Article

Environmental Economical Dispatching of Electric–Gas Integrated Energy System Considering Hydrogen Compressed-Natural Gas

Xinhui Song [1], Zhengwei Qu [1,*], Jianan Kou [1,2], Yunjing Wang [1] and Popov Maxim Georgievitch [3]

[1] Key Laboratory of Power Electronics for Energy Conservation and Drive Control, Yanshan University, Qinhuangdao 066004, China
[2] State Grid Shengzhou Power Supply Company, Shengzhou 312400, China
[3] Department of Electric Power Station and Automation of Power Systems, The Institute of Energy, Peter the Great Saint-Petersburg Polytechnic University, Saint Petersburg 195251, Russia
* Correspondence: ysu_qzw@163.com; Tel.: +0335-8074883

Abstract: As a high-quality secondary energy, hydrogen energy has great potential in energy storage and utilization. The development of power-to-hydrogen (P2H) technology has alleviated the problem of wind curtailment and improved the coupling between the power grid and the natural gas grid. Under the premise of ensuring safety, using P2H technology to mix the produced hydrogen into the natural gas network for long-distance transmission and power generation can not only promote the development of hydrogen energy but also reduce carbon emissions. This paper presents a new model for incorporating hydrogen into natural gas pipelines. To minimize the sum of wind curtailment cost, operation cost and carbon emission cost, an electric–gas integrated energy system (EGIES) model of hydrogen-compressed natural gas (HCNG) containing P2H for power generation is constructed. Aiming at the problem of global warming caused by a lot of abandoned wind and carbon emissions, the economy and environmental protection of the system model are analyzed. The results show that the model of EGIES considering HCNG can not only absorb excess wind power but also reduce carbon emission costs and system costs, which can reduce the total cost of the environmental economic dispatch of the EGIES by about 34.1%. In the context of the EGIES, the proposal of this model is of great significance to the economical and environmentally friendly operation of the system.

Keywords: electric–gas integrated energy system (EGIES); wind power consumption; power-to-hydrogen (P2H); hydrogen-compressed natural gas (HCNG)

Citation: Song, X.; Qu, Z.; Kou, J.; Wang, Y.; Georgievitch, P.M. Environmental Economical Dispatching of Electric–Gas Integrated Energy System Considering Hydrogen Compressed-Natural Gas. *Processes* **2022**, *10*, 2642. https://doi.org/10.3390/pr10122642

Academic Editors: Vladimir S. Arutyunov and Paola Ammendola

Received: 3 November 2022
Accepted: 5 December 2022
Published: 8 December 2022

1. Introduction

There has always been a misallocation of resources in China. A large amount of solar energy and wind energy is distributed in the western part, while the eastern part has mature technical conditions and greater demand for electricity [1]. How to effectively use the excess energy in the west to make up for the power supply gap in the eastern part has always been a major problem for the comprehensive development of energy and power in China. The western region is rich in renewable energy resources. It has excellent potential for developing hydrogen energy, but it is necessary to break the bottleneck of hydrogen energy storage and transportation. The current technology has preliminarily proved the feasibility of hydrogen blending in natural gas pipelines. The current national standards also allow a small proportion of hydrogen blending. Combined with the primary conditions in the western region, it is feasible to carry out hydrogen blending in natural gas pipelines. Hydrogen energy is recognized as a clean energy carrier, with the characteristics of high energy density, high conversion efficiency, no pollution and zero carbon emissions. It is considered to be the type of clean energy with the most development potential [2].

Wind energy is currently the most widely used renewable energy. However, due to the intermittency of its output, a large amount of wind power is difficult to be absorbed, and the amount of abandoned wind is too large. Power to hydrogen (P2H) [3,4] technology can convert excess wind energy into hydrogen for energy transfer, which promotes wind power consumption. The hydrogen-compressed natural gas (HCNG) model is always inseparable from the electric–gas integrated energy system (EGIES). It will be a crucial issue in the future to construct an EGIES containing HCNG and realize long-distance hydrogen transmission. The authors in [5] constructed an electricity–gas–heat integrated energy system and studied the economics of promoting wind power consumption. The authors in [6] considered the economics of adding a carbon capture system to an electrical integrated energy system. The authors in [7] proposed a variable-efficiency cogeneration scheduling model with power to gas (P2G), in which hydrogen storage was added to the water electrolysis link of P2G technology, and the use of high-grade hydrogen energy was promoted through hydrogen fuel cell cogeneration. The authors in [8] considered the cost difference between an electrolyzer and a methanation reaction tank, and the energy conversion difference between electrolyzed water and a methanation reaction in P2G production. A P2G optimal capacity planning model was proposed to reflect the hydrogen injection into the natural gas network and the investment and operation process of P2G, which further improved energy utilization efficiency. At this stage, the relevant research mainly focuses on the local coupling of the EGIES and hydrogen energy. A perfect hydrogen energy storage system has not yet been formed to realize the flexible economic dispatch between electricity and hydrogen and gas. For the natural gas network mixed with hydrogen, [9] established a simulation model coupling wind power generation, hydrogen production by electrolysis of water and natural gas pipeline network calculation. It proposed a natural gas pipeline network transportation strategy. The authors in [10] proposed that the maximum proportion of hydrogen in the mixed gas was 18%. They believed that the pipeline gas transmission power could be kept unchanged by increasing the transmission pressure after adding hydrogen. The authors in [11] modeled and evaluated the hydrogen-doped natural gas network, and obtained a maximum hydrogen-doped ratio of 6%.

In view of the above situations, based on the EGIES model, this paper uses P2H to absorb wind power for hydrogen production and adds a hydrogen storage device to construct a hydrogen production–hydrogen storage–hydrogen mixing–hydrogen power generation model. Considering the cost of the carbon tax and taking the lowest operating cost as the objective function, an EGIES model considering HCNG is established. The optimal hydrogen mixing ratio is obtained through the operation results of different hydrogen mixing ratios. The results of numerical example analysis show that the EGIES model constructed in this paper can realize the consumption of wind energy, reduce the cost of carbon emissions, ensure the economy of the system, and take into account the environmental benefits. The effect of HCNG on reducing wind curtailment, saving energy and reducing carbon, and improving the system economy is verified.

2. Construction of the EGIES Considering HCNG

Since the existing technology cannot realize the direct long-distance transportation of renewable energy, this paper proposes a new idea for the indirect transportation of renewable resources. It can be described as follows: the abandoned wind in the resource surplus area is converted into hydrogen through electrolyzers, and the produced hydrogen is injected into natural gas network nodes, so that hydrogen and natural gas can be mixed and transported to the areas with high power demand. The long-distance transportation of surplus renewable energy is realized. The structure of the EGIES considering HCNG constructed in this paper is shown in Figure 1.

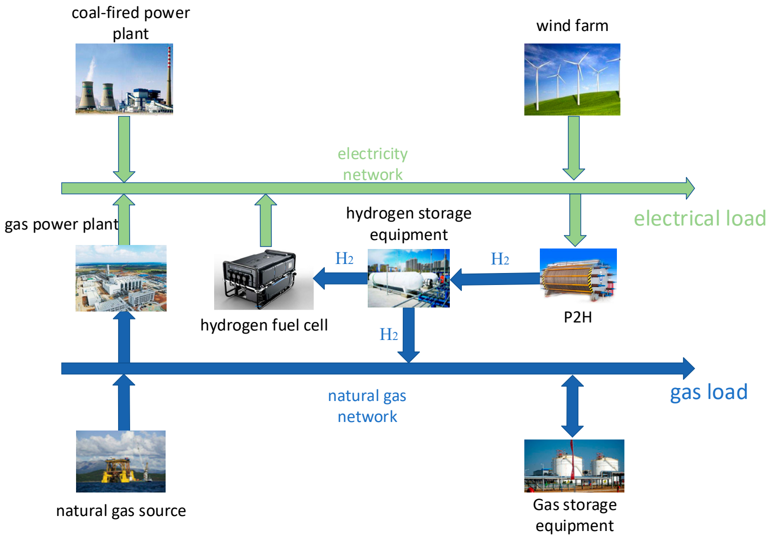

Figure 1. The structure of the EGIES considering HCNG. The green lines in the figure show the direction of the power flow from the power source to the power load, and the blue lines show the direction of the gas flow from the gas source to the gas load. "P2H" in the figure is the abbreviation of power-to-hydrogen, which means hydrogen production equipment by electrolysis of water.

2.1. P2H Model

P2H technology is to convert water into hydrogen and oxygen through electrolytic reaction, and the relational expression is as follows:

$$Q_{p2h}^{H_2} = \frac{P_{p2h}\eta_{p2h}^{H_2}\xi_{e,g}}{HHV_{H_2}} \tag{1}$$

where $Q_{p2h}^{H_2}$ is the amount of hydrogen produced by the electrolyzer, kcf/h; P_{p2h} is the input power of the electrolyzer, MW; $\eta_{p2h}^{H_2}$ is the hydrogen production efficiency of the electrolyzer; $\xi_{e,g}$ is the equivalent conversion coefficient of electric energy and heat, MBtu/MWh; and HHV_{H_2} is the calorific value of hydrogen, MBtu/kcf.

The input power constraint of the electrolyzer can be expressed as

$$I_{p2h}P_{p2h}^{\min} \leq P_{p2h} \leq I_{p2h}P_{p2h}^{\max} \tag{2}$$

where $P_{p2h}^{\min}$ and $P_{p2h}^{\max}$ are, respectively, the minimum and maximum input power of the electrolyzer, and MW; I_{p2h} is the operating state of the electrolyzer.

2.2. Hydrogen Storage Device

A hydrogen storage device is added between the outlet of the electrolyzer equipment and the natural gas source. During the wind abandoned period, the excess wind energy is converted into hydrogen storage. During the low wind period, the hydrogen can be supplied to the load through fuel cells or mixed with hydrogen into the natural gas pipeline.

Hydrogen storage devices should meet the hydrogen storage balance constraints, hydrogen storage capacity constraints, hydrogen injection flow constraints, hydrogen extraction flow constraints, and storage constraints at the beginning and end of the operation cycle. The constraint expressions are shown in Formulas (3)~(7), respectively. In addition, all the hydrogen produced by the electrolysis devices is injected into the hydrogen storage devices, which can be expressed as Formula (8).

$$E_{st}^{H_2} = E_{s,t-1}^{H_2} + \left(Q_{st}^{H_2,in} - Q_{st}^{H_2,out}\right)\Delta t \tag{3}$$

$$E_{s,\min}^{H_2} \le E_{st}^{H_2} \le E_{s,\max}^{H_2} \tag{4}$$

$$0 \le Q_{st}^{H_2,in} \le Q_{s,\max}^{H_2,in} \tag{5}$$

$$0 \le Q_{st}^{H_2,out} \le Q_{s,\max}^{H_2,out} \tag{6}$$

$$E_{s,0}^{H_2} = E_{s,NT}^{H_2} \tag{7}$$

$$Q_{st}^{H_2,in} = Q_{p2h}^{H_2} \tag{8}$$

where $E_{st}^{H_2}$ and $E_{s,t-1}^{H_2}$ are the hydrogen storage capacity of the hydrogen storage device s during t and $t-1$, respectively, kcf; $Q_{st}^{H_2,in}$ and $Q_{st}^{H_2,out}$ are the amount of hydrogen injected and taken out of the hydrogen storage device s in the t period, respectively, kcf/h; $E_{s,\min}^{H_2}$ and $E_{s,\max}^{H_2}$ are the minimum hydrogen storage capacity and capacity of the hydrogen storage device s, respectively, kcf; $Q_{s,\max}^{H_2,in}$ and $Q_{s,\max}^{H_2,out}$ are the maximum amount of hydrogen injected and withdrawn from the hydrogen storage device s, respectively, kcf/h; $E_{s,0}^{H_2}$ and $E_{s,NT}^{H_2}$ are the hydrogen amount of the hydrogen storage device s at the initial period and the end period of the operation cycle, respectively, kcf; time step equals to 1 h; and N_T is the end period of the operation cycle.

2.3. Flexible Hydrogen Doping Mode

During the wind abandoned period, the surplus electricity of the wind farm produces hydrogen through the electrolyzer and stores it in the hydrogen storage devices. During the low wind period, the hydrogen in the hydrogen storage devices supplies power to the grid through the hydrogen fuel cell (HFC).

However, when the amount of abandoned wind is huge and the capacity of the hydrogen storage devices reaches the upper limit, in order to further reduce the abandoned wind, the excess hydrogen is injected into the natural gas network nearby, and mixed with natural gas as the gas source and transported to areas with high electricity demand. In order to make the hydrogen doping mode more flexible and efficient, the hydrogen doping rate can be changed within a feasible range according to the specific unit output combination and load conditions in each period, so as to obtain better results. The corresponding relationship can be written as

$$Q_{st}^{H_2,out} = Q_{hfc,t} + Q_{ht} \tag{9}$$

$$\begin{cases} Q_{ht} = \alpha Q_{\omega t} \\ 0 \le \alpha \le 0.2 \end{cases} \tag{10}$$

where $Q_{hfc,t}$ is the hydrogen injection amount of the hydrogen fuel cell in the t period, kcf/h; Q_{ht} is the amount of hydrogen doped into the natural gas network, kcf/h; α is the hydrogen doping ratio; and $Q_{\omega t}$ is the gas production of natural gas wells in the t period, kcf/h.

Calculating the replacement amount of hydrogen for natural gas by generating the same electric energy, the relationship can be expressed as

$$Q_{ht} = 3Q_{NG,t}^{replace} \tag{11}$$

where $Q_{NG,t}^{replace}$ is the amount of natural gas replaced by hydrogen, kcf/h.

The HFC power generation model can be described as

$$Q_{hfc,t} = \left(\psi\left(P_{hfc,t}\right) + SU_{hfc,t} + SD_{hfc,t}\right)/HHV_{H_2} \tag{12}$$

where $SU_{hfc,t}$ and $SD_{hfc,t}$ are the power consumption of the hydrogen fuel cell on and off during the period, respectively, MBtu; $P_{hfc,t}$ is the output power of the hydrogen fuel cell during the t period, MW; $\psi\left(P_{hfc,t}\right)$ is the effective energy consumption of hydrogen fuel cell during the t period, MBtu; and HHV_{H_2} is the calorific value of hydrogen, MBtu/kcf.

3. Dispatch Model of the EGIES Considering HCNG

3.1. Objective Function

The environmental economic dispatching objective of the EGIES is to minimize the total cost. The total cost consists of three parts: operation cost, carbon emission cost and wind abandonment penalty cost, so the relationship can be written as

$$\min F = F_1 + F_2 + F_3 \tag{13}$$

where F, F_1, F_2 and F_3 are the total cost, operation cost, carbon tax cost and wind abandonment penalty cost, respectively.

The operating cost includes the power generation cost and start–stop cost of coal-fired units, the gas production cost of natural gas wells and the gas consumption cost of hydrogen storage devices. Among them, the relationship between fuel consumption and output power in the power generation process of coal-fired units can be expressed as

$$\psi(P_{it}) = c + bP_{it} + aP_{it}^2 \tag{14}$$

$$F_1 = \sum_{t\in\Omega_T}\left\{\begin{array}{l}\sum\limits_{i\in\Omega_{CU}}\rho_i[\psi(P_{it}) + SU_{it} + SD_{it}] \\ + \sum\limits_{\omega\in\Omega_{GW}}\rho_\omega Q_{\omega t} + \sum\limits_{s\in\Omega_{HS}}\rho_s Q_{st}^{H_2,out}\end{array}\right\} \tag{15}$$

where Ω_T and Ω_{CU} are the dispatch period and coal-fired unit set, respectively; Ω_{GW} and Ω_{HS} are natural gas wells and hydrogen storage devices, respectively; P_{it} is the output power of the unit i during the t period, MW; $\psi(P_{it})$ is the effective fuel energy consumption of the unit i during the t period, MBtu; SU_{it} and SD_{it} are the energy consumption of the unit i on and off during the t period, respectively, MBtu; and ρ_i, ρ_ω and ρ_s are the fuel price of the unit i, the unit gas production cost of natural gas well ω, and the unit gas consumption cost of gas storage devices S, respectively, USD/MBtu, USD/kcf and USD/kcf.

The carbon emission cost can be expressed as

$$F_2 = \sum_{t\in\Omega_T}\rho_{ct}[\sum_{i\in\Omega_{CU}}\mu_i P_{it} + \sum_{i\in\Omega_{GU}}\mu_j P_{it}^{NG}] \tag{16}$$

where Ω_{GU} is the set of gas-fired units; μ_i is the carbon emission intensity of coal-fired units, kcf/MWh; μ_j is the carbon emission intensity of gas-fired units, kcf/MWh; P_{it}^{NG} is the output power of natural gas in gas-fired units, MW; and ρ_{ct} is the carbon tax price, USD/kcf.

The wind abandonment penalty cost is proportional to the difference between the wind power forecast value and the on-grid value of wind power, which can be expressed as

$$F_3 = \sum_{t\in\Omega_T}\sum_{w\in\Omega_{WF}}\rho_w(P_{wt}^f - P_{wt}) \tag{17}$$

where Ω_{WF} is the collection of wind farms; ρ_w is the wind abandonment penalty price, USD/MWh; and P_{wt}^f and P_{wt} are the forecasted power and grid-connected power of the w wind farm during the t period, respectively, MW.

3.2. Constraints

3.2.1. Power System Constraints

High-voltage transmission lines use the DC power flow method to calculate the active power distribution, ignoring network losses. In order to ensure the real-time balance of power transmission, the net injected power of each node is equal to the transmission power of the transmission line connecting the node. The corresponding line transmission power constraints are as follows:

$$\begin{cases} \sum\limits_{i\in\Omega_{FU}} A_{bi}P_{it} + \sum\limits_{w\in\Omega_{WF}} A_{bw}P_{wt} - \\ \sum\limits_{p2h\in\Omega_{P2H}} A_{b,p2h}P_{p2h,t} - EL_{bt} = \sum\limits_{l\in\Omega_{TL}} A_{bl}PL_{lt} \\ PL_{lt} = (\theta_{l1,t} - \theta_{l2,t})/x_l \\ PL_{l,\min} \le PL_{lt} \le PL_{l,\max} \\ \theta_{b,\min} \le \theta_{bt} \le \theta_{b,\max} \\ \theta_{ref} = 0 \end{cases} \tag{18}$$

where Ω_{WF}, Ω_{FU}, Ω_{P2H} and Ω_{TL} are the collection of wind farms, fuel units, P2H devices and transmission lines, respectively; $A_{b(\cdot)}$ is the node correlation matrix value corresponding to the power node b; EL_{bt} is the electrical load of the node b during the t period, MW; PL_{lt} is the transmission power of the line l during the t period, MW; $\theta_{l1,t}$ and $\theta_{l2,t}$ are the voltage angles of the head-end node l_1 and the tail-end node l_2 of the line l during the t period, respectively, rad; x_l is the reactance of the line l, pu; $PL_{l,\max}$ and $PL_{l,\min}$ are the upper and lower limits of the active power transmitted by the line l, MW; $\theta_{b,\min}$ and $\theta_{b,\max}$ are the minimum and maximum value of the node b voltage angle, respectively, rad; and θ_{ref} and θ_{bt} are the voltage angle of the reference node and the voltage angle of the node b during the t period, respectively, rad.

System constraints also include the power balance constraint shown in Formula (19), and the positive and negative spinning reserve constraints shown in Formula (20). Constraints for fossil fuel units include the output power constraints shown in Formulas (21) and (22), the ramp constraints shown in Formula (23), the start–stop energy consumption constraints shown in Formulas (24) and (25), and the minimum start–stop time constraints shown in Formula (26).

$$\sum_{i\in\Omega_{FU}} P_{it} + \sum_{w\in\Omega_{WF}} P_{wt} = \sum_{L\in\Omega_{EL}} P_{Lt} + \sum_{p2h\in\Omega_{P2H}} P_{p2h,t} \tag{19}$$

$$\begin{cases} \sum\limits_{i\in\Omega_{FU}} P_{i,\max}I_{it} + \sum\limits_{w\in\Omega_{WF}} P_{wt} \ge \sum\limits_{L\in\Omega_{EL}} P_{Lt} + SR_t^{up} \\ \sum\limits_{i\in\Omega_{FU}} P_{i,\min}I_{it} + \sum\limits_{w\in\Omega_{WF}} P_{wt} \le \sum\limits_{L\in\Omega_{EL}} P_{Lt} - SR_t^{down} \end{cases} \tag{20}$$

$$I_{it}P_{i,\min} \le P_{it} \le I_{it}P_{i,\max}, i \in \Omega_{FU} \tag{21}$$

$$P_{it} = P_{it}^{NG} + P_{it}^{H_2}, i \in \Omega_{GU} \tag{22}$$

$$\begin{cases} P_{it} - P_{i,t-1} \ge R_i^{up} I_{i,t-1} + \\ \qquad P_{i,\max}(1 - I_{it}) + P_{i,\min}(I_{it} - I_{i,t-1}) \\ P_{i,t-1} - P_{it} \ge R_i^{down} I_{it} + \\ \qquad P_{i,\max}(1 - I_{i,t-1}) + P_{i,\min}(I_{i,t-1} - I_{it}) \end{cases}, i \in \Omega_{FU} \tag{23}$$

$$\begin{cases} SU_{it} \ge su_i(I_{it} - I_{i,t-1}) \\ SU_{it} \ge 0 \end{cases}, i \in \Omega_{FU} \tag{24}$$

$$\begin{cases} SD_{it} \ge sd_i(I_{i,t-1} - I_{it}) \\ SD_{it} \ge 0 \end{cases}, i \in \Omega_{FU} \tag{25}$$

$$\begin{cases} (T_{i,t-1}^{on} - T_{i,\min}^{on})(I_{i,t-1} - I_{it}) \ge 0 \\ (T_{i,t-1}^{off} - T_{i,\min}^{off})(I_{it} - I_{i,t-1}) \ge 0 \end{cases}, i \in \Omega_{FU} \tag{26}$$

where Ω_{EL} is the set of electrical loads; P_{Lt} is the electrical load during the t period, MW; SR_t^{up} and SR_t^{down} are the upper and lower rotation reserve requirements of the system during the t period, respectively, MW; $P_{i,\min}$ and $P_{i,\max}$ are the minimum and maximum output power of the unit i, respectively, MW; I_{it} is the running state of the unit i during the t period; P_{it}^{NG} and $P_{it}^{H_2}$ are the output power of the natural gas part and the hydrogen part of the gas unit i, respectively, MW; R_i^{up} and R_i^{down} are the up and down ramp rates of the unit i, respectively, MW; SU_{it} and SD_{it} are the energy consumption of the unit i on and off during the t period, respectively, MBtu; su_i and sd_i are the energy consumption of the unit i on startup and shutdown, respectively, MBtu; $T_{i,\min}^{on}$ and $T_{i,\min}^{off}$ are the minimum start and stop time of the unit i, respectively, h; and $T_{i,t-1}^{on}$ and $T_{i,t-1}^{off}$ are the continuous start and stop time of the unit i before the $t-1$ period, respectively, h.

3.2.2. Natural Gas Constraints

The natural gas system comprises gas wells, pipelines, compressors, gas storage devices and loads. The corresponding system structure can be briefly described in Figure 2. The commonly used steady-state model of the natural gas system [12,13] is given as follows:

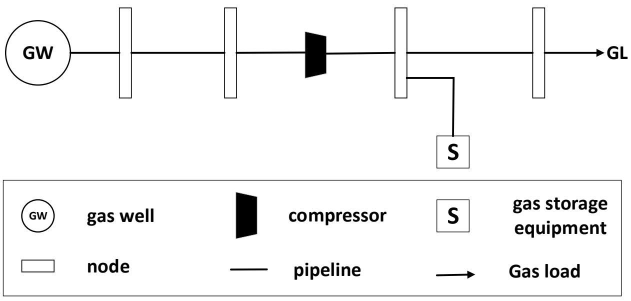

Figure 2. Natural gas system. In the figure, "GW" is the abbreviation of gas well, which means the source of natural gas production; "GL" is the abbreviation of gas load, which means the load of the natural gas system; "S" is the abbreviation of gas storage equipment, which means the storage equipment of the natural gas system; the white rectangles represent the nodes in the natural gas system; the black line represents the pipeline in the natural gas system; the black trapezoid represents the compressor in the natural gas system.

It can be seen from Figure 2 that gas wells are the source of natural gas production, and the output natural gas flow should meet the following constraint.

$$Q_{\omega,\min} \le Q_{\omega t} \le Q_{\omega,\max} \tag{27}$$

where $Q_{\omega,\min}$ and $Q_{\omega,\max}$ are the minimum and maximum gas production flow rates of natural gas wells, respectively, kcf/h.

Gas wells are generally located far from the load area, and the natural gas produced is mainly piped to the load. During natural gas transmission, pressurization stations are typically installed along the pipeline every 50–100 miles to compensate for pressure losses caused by pipeline friction. Therefore, natural gas pipelines can be divided into ordinary pipelines and compressor pipelines according to whether a compressor is configured. The natural gas flow transmitted by ordinary pipelines is related to the nodal pressure at both ends of the pipeline, which is usually expressed by the Weymouth equation [14], as shown in Equation (28). At the same time, the transmission direction of natural gas in ordinary pipelines depends on the node pressure at both ends of the pipeline. It is from high-pressure nodes to low-pressure nodes, as shown in Equation (29).

$$Q_{pt} = \mathrm{sgn}(pr_{p1,t}, pr_{p2,t}) C_p \sqrt{\left| {pr^2}_{p1,t} - {pr^2}_{p2,t} \right|}, p \in \Omega_{PP} \tag{28}$$

$$\mathrm{sgn}(pr_{p1,t}, pr_{p2,t}) = \begin{cases} +1, pr_{p1,t} \ge pr_{p2,t} \\ -1, pr_{p1,t} \le pr_{p2,t} \end{cases} \tag{29}$$

where $pr_{p1,t}$ and $pr_{p2,t}$ are the pressure values of the first node $p1$ and the end node $p2$ of the pipeline p during the t period, respectively, Psig; Ω_{PP} is a collection of ordinary pipes; C_p is the pipeline constant, which depends on the length, diameter, friction and gas composition, kcf/Psig; and Q_{pt} is the natural gas flow through the pipeline p during the t period, kcf/h.

Similar to the transformer in the power system, the compressor piping is used to improve pressure levels in natural gas systems. The input node pressure of the compressor pipeline can be smaller than the output node pressure, and the corresponding model can be described as

$$M_{p,\min} pr_{p1,t} \leq pr_{p2,t} \leq M_{p,\max} pr_{p1,t}, p \in \Omega_{AP} \tag{30}$$

where $M_{p,\min}$ and $M_{p,\max}$ are the minimum and maximum compression ratios of the compressor pipeline p, respectively; and Ω_{AP} is a collection of compressor pipes.

In addition, for the natural gas system, the node pressure constraint is shown in Formula (31), the node supply and demand balance constraint are shown in Formula (32), and the gas consumption constraints are shown in Formula (33).

$$pr_{n,\min} \leq pr_{nt} \leq pr_{n,\max} \tag{31}$$

$$\begin{aligned} &\sum_{\omega \in \Omega_{GW}} B_{n\omega} Q_{\omega t} + \sum_{s \in \Omega_{HS}} B_{ns} \left(Q_{st}^{H_2,out} - Q_{st}^{H_2,in} \right) \\ &- \sum_{i \in \Omega_{GU}} B_{ni} Q_{it} - \sum_{hfc \in \Omega_{HFC}} B_{n,hfc} Q_{hfc,t} \\ &- GL_{nt} = \sum_{p \in \Omega_{GP}} B_{np} Q_{pt} \end{aligned} \tag{32}$$

$$\begin{cases} Q_{it}^{NG} = \left(\psi\left(P_{it}^{NG}\right) + SU_{it} + SD_{it} \right) / HHV_{NG} \\ Q_{it}^{H_2} = \left(\psi\left(P_{it}^{H_2}\right) + SU_{it} + SD_{it} \right) / HHV_{H_2} \\ i \in \Omega_{GU} \end{cases} \tag{33}$$

where Ω_{HFC} and Ω_{GP} are the HFC collection and the natural gas pipeline collection, respectively; $pr_{n,\min}$ and $pr_{n,\max}$ are the minimum and maximum pressures of the node n, respectively, Psig; $B_{n(\cdot)}$ is the node association matrix value corresponding to the natural gas node n; pr_{nt} is the pressure of the node n during the t period, Psig; GL_{nt} is the gas load of the natural gas node n during the t period, kcf/h; Q_{it}^{NG} and $Q_{it}^{H_2}$ are the gas consumption of the natural gas part and the hydrogen part of the gas unit i during the t period, respectively, kcf/h; and HHV_{NG} is the calorific value of natural gas, MBtu/kcf, sized 1.026.

From Formulas (9)–(11), the constraints of gas turbine combustion of natural gas and hydrogen blended gas can be obtained, as shown below.

$$Q_{it}^{H_2} = \alpha Q_{it}^{NG} \tag{34}$$

$$\begin{aligned} &\tfrac{1}{3}\Big(\sum_{s \in \Omega_{HS}} Q_{st}^{H_2,out} - \sum_{hfc \in \Omega_{HFC}} Q_{hfc,t} - \sum_{i \in \Omega_{GU}} Q_{it}^{H_2} \Big) \\ &\quad + \Big(\sum_{\omega \in \Omega_{GW}} Q_{\omega t} - \sum_{i \in \Omega_{GU}} Q_{it}^{NG} \Big) = \sum_{n \in \Omega_{GL}} GL_{nt} \end{aligned} \tag{35}$$

where Ω_{GL} is the gas load collection.

3.3. Model Solution

It can be seen from the above modeling process that the constructed environmental economic dispatch model of the EGIES contains both continuous variables and integer variables. At the same time, it can be seen from Formulas (14) and (28) that the fuel consumption characteristic equation of the unit is a quadratic form, and the natural gas flow equation of an ordinary pipeline is a non-convex and nonlinear form. Therefore, the model is a mixed integer nonlinear programming problem, and it is difficult to obtain the global optimal solution by traditional mathematical methods. The incremental linearization method can be used for processing. Firstly, the nonlinear equation is linearized. Then the model is transformed into a mixed integer linear programming problem. Finally, the CPLEX solver is used to solve the problem.

Linearization of Nonlinear Equations

After using the nodal pressure values $pr_{p1,t}$ and $pr_{p2,t}$ to replace the square values ${pr^2}_{p1,t}$ and ${pr^2}_{p2,t}$, Equation (28) can be rewritten as

$$Q_{pt}|Q_{pt}| = C_p^2(pr_{p1,t} - pr_{p2,t}), p \in \Omega_{PP} \tag{36}$$

It can be seen from the observation that Equation (36) has been transformed into a linear form, and Equations (36) and (14) are both univariate quadratic equations, which can be processed by the incremental piecewise linearization method [15] with a faster calculation speed. As shown in Figure 3, the model of incremental piecewise linearization is given and the original curves are replaced by differential straight lines, so that the nonlinear programming problem is transformed into a linear programming problem. Finally, use the Yalmip toolkit of Matlab to call the Cplex solver to solve the mixed integer linear programming problem.

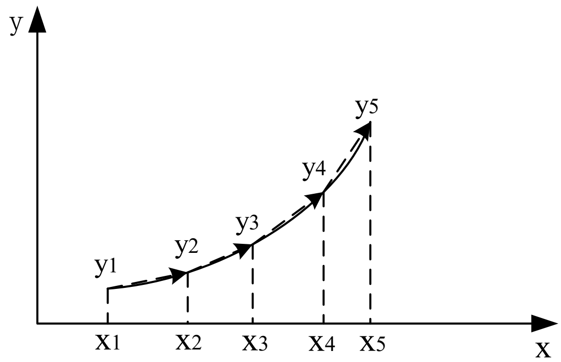

Figure 3. Schematic diagram of piecewise linearization. In the figure, the curve described by the dotted line represents the original nonlinear curve; "(X1,y1)-(X5,y5)" represents several coordinate points on the original nonlinear curve; the lines with arrows represent the differential lines for incremental piecewise linearization of the original curve.

4. Results and Discussion

The 6-node power system and the 7-node natural gas system [16] are shown in Figure A1 of Appendix A. The 6-node power system includes two gas-fired units "G1-G2", three coal-fired units "G3-G5", one wind farm "W", one P2H equipment "P2H", seven transmission lines and three electrical loads "EL1-EL3". Both the wind farm "W" and the P2H equipment "P2H" are installed on power node 4. The 7-node natural gas system includes two natural gas wells "GW1-GW2", one compressor represented by a black trapezoid, one gas storage device "S", six natural gas pipelines and three gas loads "GL1-GL3". The power system and the natural gas system are mainly coupled by the gas-fired units "G1-G2" and the P2H equipment "P2H". The gas-fired units "G1-G2" are supplied by natural gas node 3 and natural gas node 1, respectively. Part of the hydrogen generated from P2H conversion is supplied to the fuel cell for power generation, and part of the hydrogen is mixed with natural gas and enters the natural gas pipeline.

The upper and lower spinning reserve demand in each period of the power system is set at 10% of the total load, and the carbon tax price is 5 USD/t. The maximum and minimum injection power of the P2H equipment are 100 MW and 10 MW, respectively. The capacity of the hydrogen storage device in the additional device matches the maximum injection power of the P2H equipment. The maximum and minimum output power of the HFC are 20 MW and 2 MW, respectively. The hydrogen production efficiency $\eta_{p2h}^{H_2}$ of the electrolyzer is 0.73. The equivalent conversion coefficient $\eta_{p2h}^{H_2}$ of electric energy and heat is 3.41. The high calorific value HHV_{H_2} of hydrogen is 0.342. The predicted values of the electric load, gas load and wind power are shown in Figure 4, and the corresponding peak values are 576.19 MW, 1835.5 kcf/h and 200.27 MW, respectively. Other system parameters, such as units, gas wells, power nodes, natural gas nodes, power lines, and natural gas pipelines are shown in Tables A1–A7 in Appendix A.

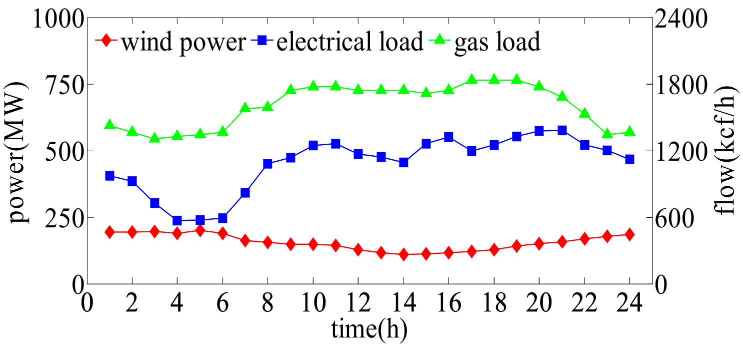

Figure 4. Forecast values of electricity load, gas load and wind power. In the figure, the green curve drawn by the triangle connection represents the forecast values of gas load; the blue curve drawn by the square connection represents the forecast values of electricity load; the red curve depicted by the diamond connection represents the wind power forecast values.

In order to verify the validity of the model, the four cases are set as follows:

Case 1: Environmental and economic dispatch of the EGIES without considering P2H equipment.

Case 2: Based on Case 1, P2H and HFC equipment are added, but hydrogen is not mixed into the natural gas pipeline.

Case 3: Based on Case 1, P2H equipment is added, and the case where hydrogen is mixed into the natural gas pipelines is the only one considered.

Case 4: Based on Case 2, the case where hydrogen is mixed into the natural gas pipeline is added.

Among them, Case 1 is used as the basic case. The hydrogen produced in Case 2 is all used for HFC power generation. The hydrogen produced in Case 3 is all used for mixing into the natural gas pipelines. The hydrogen produced in Case 4 can not only be used for HFC power generation, but also be mixed with hydrogen into natural gas pipelines. Its hydrogen doping mode is more flexible.

4.1. Optimization Results and Analysis

Figure 5 shows the output of each unit in Cases 1–4. It can be seen that the output of the gas-fired units in Cases 3 and 4 accounts for a larger proportion of the total unit output than that of Cases 1 and 2. Since both Cases 3 and 4 consider the hydrogen mixing mode, hydrogen mixing can effectively increase the output of gas-fired units. The greater the output of gas-fired units, the lower the cost of carbon emissions. This indicates that the hydrogen mixing mode is helpful for reducing carbon emissions.

The various costs of the objective function in Cases 1–4 are shown in Table 1. It can be seen that compared with Cases 1–3, Case 4 has the lowest total cost, operating cost, carbon emission cost and wind power reduction cost. The superiority of the hydrogen-mixed operation mode to improve the environmental and economic dispatch of the EGIES is verified. Both P2H power generation and HCNG can reduce natural gas supply and provide new ideas for future hydrogen energy transportation.

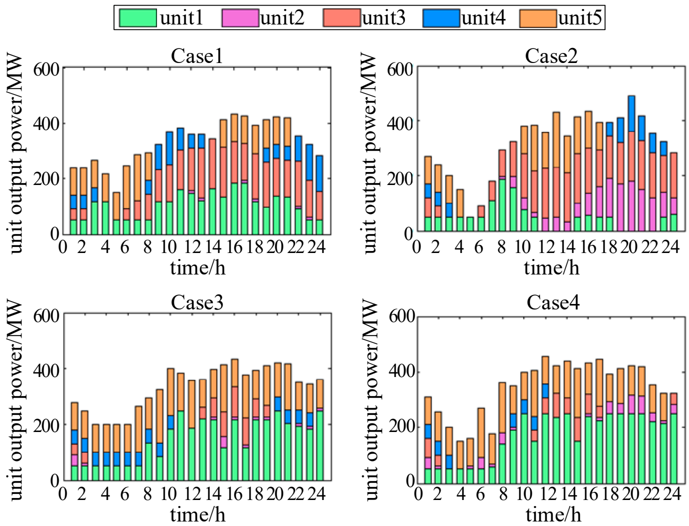

Figure 5. Output of each unit in Cases 1–4. In the figure, the green histograms represent the output of unit 1, which means the output of the first gas-fired unit. The purple histograms represent the output of unit 2, which means the output of the second gas-fired unit. The red histograms represent the output of unit 3, which means the output of the first coal-fired unit. The blue histograms represent the output of unit 4, which means the output of the second coal-fired unit. The orange histograms represent the output of unit 5, which means the output of the third coal-fired unit.

Table 1. Costs of objective functions in Cases 1–4.

Case	Total Cost/USD	Fuel Cost/USD	Carbon Tax Cost/USD	Wind Abandonment Penalty Cost/USD
1	660,961.27	459,645.22	114,486.38	86,829.67
2	583,590.90	452,978.90	95,494.67	35,117.33
3	539,374.13	376,531.29	109,092.18	53,750.66
4	435,415.79	111,975.03	63,608.53	259,832.23

4.2. Wind Power Reduction Results and Analysis

Figure 6 shows the reduction in wind power in each period in Cases 1–4. It can be seen that wind power reduction occurs during periods 1–7 and 17 in Case 1. After adding P2H equipment, Cases 2–4 will reduce the amount of wind power reduction. However, Case 2 only has HFC power generation, and Case 3 only has HCNG, so the reduction is not as obvious as Case 4. In Case 4, both HFC power generation and HCNG are used to promote wind power consumption.

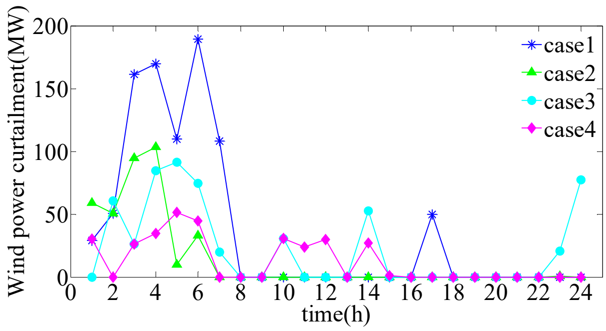

Figure 6. Hourly wind power curtailment. In the figure, the blue curve drawn by asterisk connection, the green curve drawn by triangle connection, the cyan curve drawn by circular connection and the purple curve drawn by diamond connection, respectively, represent the wind power curtailment of Case 1, Case 2, Case 3 and Case 4.

In order to analyze the operation of the P2H equipment, Figure 7 shows the input power of the P2H equipment, and the graph of the amount of hydrogen produced by the P2H equipment is consistent with it. It can be seen from Figure 7 that in Case 2, the P2H equipment is started only in periods 10, 13, 17 and 20. In Case 3, the P2H equipment is started in periods 1 and 3–7. In Case 4, the P2H equipment is started in more than half of the periods. Compared with Case 2 and Case 3, both the number of periods and the total input power of P2H input power are significantly increased in Case 4, so the consumption of wind power is significantly increased, the cost of wind curtailment is significantly reduced, and the goal of absorbing wind power and reducing wind curtailment is achieved.

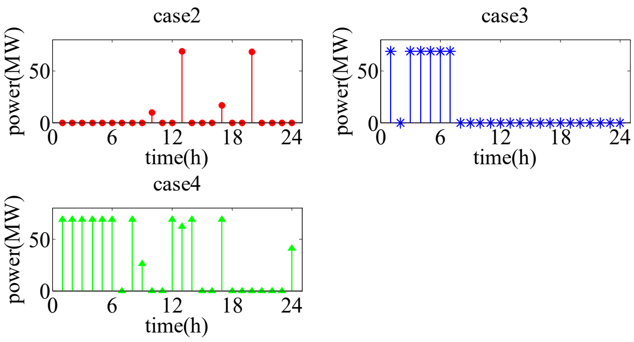

Figure 7. Input power of P2H equipment in Cases 2–4. In the figure, the red circulars, the blue asterisks and the green triangles, respectively, represent the input power of the P2H equipment in Case 2, Case 3 and Case 4.

4.3. Analysis of Hydrogen Doping Results

The hydrogen produced in Case 3 is all used for hydrogen mixing, and the hydrogen produced in Case 4 is mixed with hydrogen in a flexible hydrogen mixing mode. The results of the hydrogen mixing amount obtained by both are shown in Figure 8. It can be seen from Figure 8 that in Case 3, the hydrogen mixing amount in periods 1–7 and 23 is zero, and in Case 4, the hydrogen mixing amount in periods 1–9 and 12–15 is zero. Overall, since the hydrogen in Case 3 is all used for hydrogen mixing, the amount of hydrogen mixed in Case 3 is larger than that in Case 4. It can be seen from Figures 6 and 7 that the production of hydrogen by the P2H equipment and the addition of hydrogen into the natural gas pipeline are not synchronized in time. Due to the addition of hydrogen storage equipment, hydrogen mixing transportation will not be limited by the time of hydrogen production, and hydrogen mixing has greater flexibility in time.

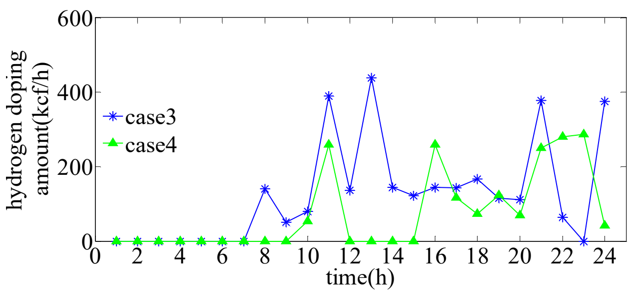

Figure 8. Comparison of the amount of hydrogen mixed in Case 3 and Case 4. In the figure, the blue curve drawn by asterisk connection represents the amount of hydrogen mixed in Case 3; the green curve drawn by triangle connection represents the amount of hydrogen mixed in Case 4.

Figure 9 is the comparison of the hydrogen mixing rate between Case 3 and Case 4. It can be seen from Figure 9 that the hydrogen mixing rate of Case 3 remains at 0.2 in other hydrogen doping periods except for period 7, which is greatly affected by the constraint of the hydrogen mixing rate. In comparison, the hydrogen mixing rate of Case 4 has a large variability during the hydrogen mixing period and is less affected by the constraint of the hydrogen mixing rate.

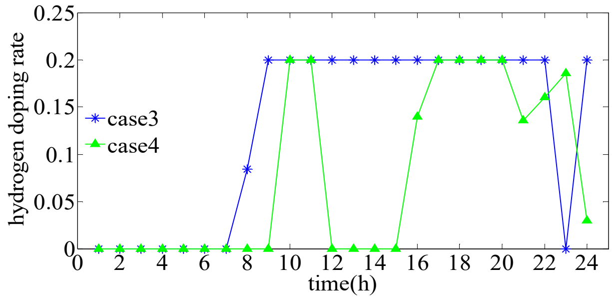

Figure 9. Comparison of hydrogen mixing rate between Case 3 and Case 4. In the figure, the blue curve drawn by asterisk connection represents the hydrogen mixing rate of Case 3; the green curve drawn by triangle connection represents the hydrogen mixing rate of Case 4.

4.4. Sensitivity Analysis

The carbon tax price and hydrogen mixing rate are important factors affecting the environmental economic dispatch of hydrogen-infused EGIES. Based on the hydrogen mixing rate, the total costs of Cases 1–4 under different carbon tax prices are shown in Figure 10, and the operating results of Case 4 under different hydrogen mixing rates are shown in Figure 11.

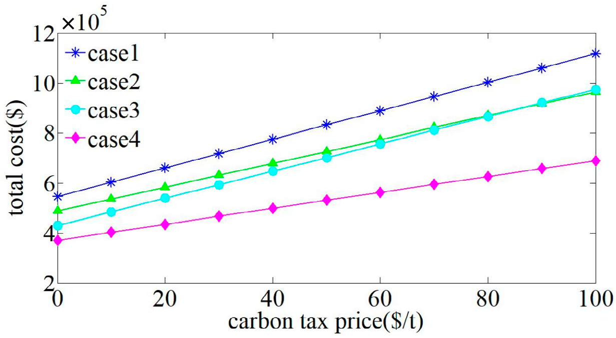

Figure 10. The total cost under different carbon tax prices in Cases 1–4. In the figure, the blue curve drawn by asterisk connection, the green curve drawn by triangle connection, the cyan curve drawn by circular connection and the purple curve drawn by diamond connection, respectively, represent the total cost under different carbon tax prices in Case 1, Case 2, Case 3 and Case 4.

It can be seen from Figure 10 that with the increase in carbon tax price, the total cost of Cases 1–4 also increases, but the growth slopes are different. Compared with Case 1, under different carbon tax prices, P2H equipment or HCNG can reduce the total cost of environmental economic dispatch of the EGIES in Cases 2–4. As far as the growth slope is concerned, the slopes of Case 1 and Case 3 are almost the same, and both are larger than those of Case 2 and Case 4. When the carbon tax is 90 USD/t, the total cost of Case 3 starts to be larger than that of Case 2, while the slope of Case 4 is obviously smaller. It is not hard to see that with the carbon tax price increasing, the total cost of Case 4 will be far less than the other cases.

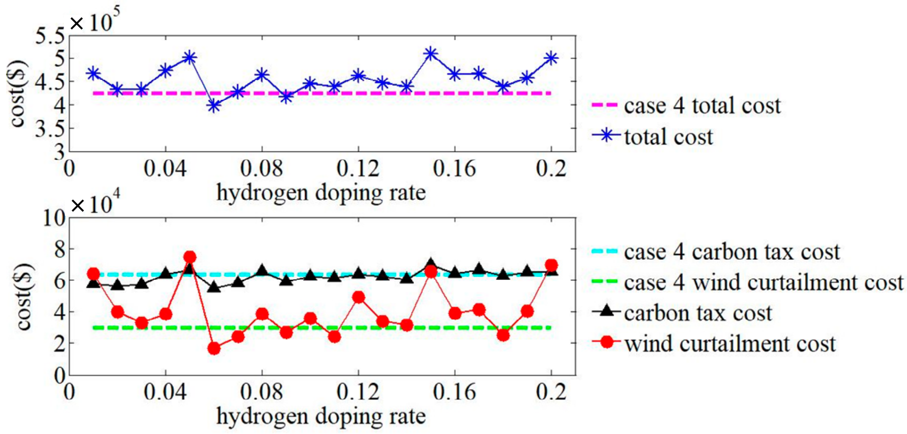

Figure 11. Operation results of different hydrogen mixing rates in Case 4. In the figure, the blue curve drawn by asterisk connection, the black curve drawn by triangle connection and the red curve drawn by circular connection, respectively, represent the total cost, the carbon tax cost and the wind abandonment cost of Case 4 under different hydrogen mixing rates. The purple dotted line, the blue dotted line and the green dotted line, respectively, represent the total cost value, the carbon tax cost value and the wind abandonment cost value of Case 4 under the flexible hydrogen mixing model.

Within the constraint range of the hydrogen mixing rate, the hydrogen mixing rate for each period is set to a fixed value. With the increase in the fixed value of the hydrogen mixing rate, the changes in the total cost, carbon tax cost and wind abandonment cost of Case 4 are shown in Figure 11. It can be seen from Figure 11 that with the increase in the fixed value of the hydrogen mixing rate, there is no linearity and monotonicity in the changes in various costs. This is because the hydrogen mixing rate in 24 periods is set as a fixed value, and the changes in the combined output of units, gas production from gas wells, electrical load and gas load in each period are not considered. The hydrogen mixing mode is not flexible. The three straight lines in Figure 11 are the three cost values under the flexible hydrogen mixing mode of Case 4. The hydrogen mixing rate results from the combined effect of various changes in the source and charge of electricity and gas within the limited range. The rate in each period is shown in Figure 9.

It can also be seen from Figure 11 that the total cost, carbon tax cost and wind abandonment cost, respectively, represent the three indicators of economy, environmental protection and wind curtailment consumption of the dispatching model. In general, only when the hydrogen mixing rate in each period is set at 0.06 and 0.09 are the comprehensive three indicators optimal.

5. Conclusions

In order to improve the wind power consumption capacity and reduce the cost of carbon emissions, this paper proposes an EGIES environmental economic dispatch model of HCNG containing P2H. It then converts the model into a mixed integer linear programming problem to solve. The simulation results show that adding P2H and HCNG to the EGIES can absorb excess wind power and reduce the total cost of environmental economic dispatch of the EGIES by about 34.1%. In addition, the total cost of environmental economic dispatch of the constructed EGIES model is more sensitive to the carbon tax price. With the increase in carbon tax price, the advantages of environmental economic dispatch of EGIES will become more obvious. With the increase in the hydrogen mixing ratio, the hydrogen mixing mode proposed in this paper provides a new idea for the long-distance transportation of hydrogen and promotes the development of hydrogen energy.

However, the current work of this paper still has limitations, mainly because the EGIES, which uses P2H and HCNG technologies to store, transport and transform energy, still have a single form of energy storage, and the system energy conversion efficiency and economy are still not ideal. Therefore, the future work direction will focus on how to apply multi-type energy storage technology to the overall planning and scheduling of the IES based on the carbon perspective, so as to improve the overall energy efficiency, economy, environmental protection and other comprehensive indicators of the system.

Author Contributions: Conceptualization, Z.Q.; methodology, X.S.; software, J.K.; validation, X.S., Z.Q. and J.K.; formal analysis, X.S.; investigation, J.K.; resources, Z.Q. and Y.W.; data curation, Y.W.; writing—original draft preparation, J.K. and X.S.; writing—review and editing, X.S. and Z.Q.; supervision, Z.Q. and Y.W. and P.M.G. All authors have read and agreed to the published version of the manuscript.

Funding: This research received no external funding.

Institutional Review Board Statement: Not applicable.

Informed Consent Statement: Not applicable.

Data Availability Statement: The data presented in this study are available on request from the corresponding author. The data are not publicly available due to privacy restrictions.

Acknowledgments: All authors thank the editor and anonymous reviewers for their constructive comments and suggestions to improve the quality of this paper.

Conflicts of Interest: The authors declare no conflict of interest.

Appendix A

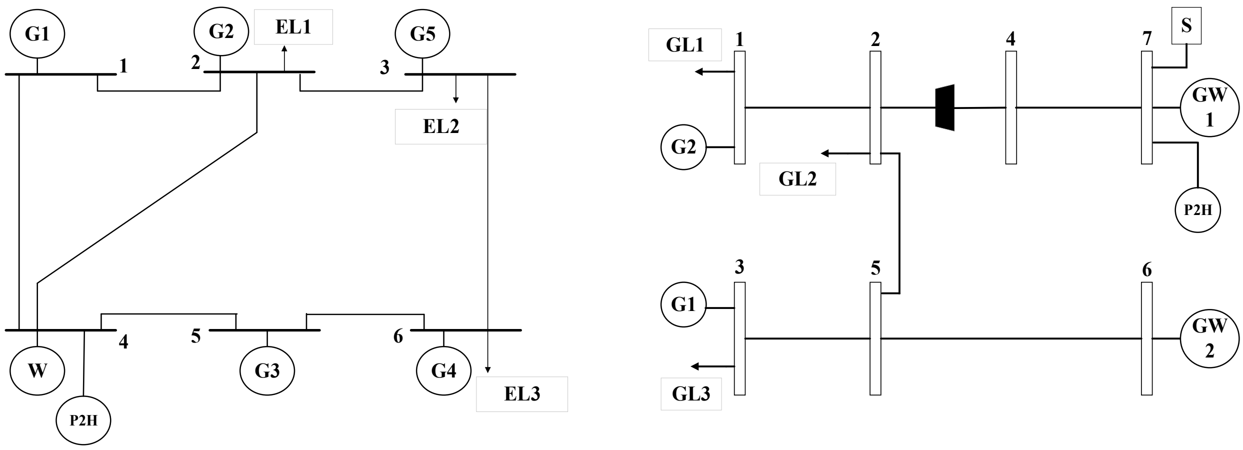

Figure A1. Node diagram of 6-node power system and 7-node natural gas system.

Table A1. Cost parameters of generators.

Unit	a_i/(MBtu/MW2h)	b_i/(MBtu/MWh)	c_i/MBtu	SU_i/MBtu	SD_i/MBtu	ρ_i/(USD/MBtu)
G1	0.0024	12.33	28	120	0	2.5
G2	0.008	14.51	42	30	0	2.5
G3	0.0459	15.47	74.33	40	0	2.5
G4	0.0128	17.82	10.15	50	0	2.5
G5	0.0044	13.29	39	100	0	2.5

Table A2. Technology parameters of generators.

Unit	$P_{i,\min}$/MW	$P_{i,\max}$/MW	R_i^{up}/MW	R_i^{down}/MW	$T_{i,\min}^{on}$/h	$T_{i,\min}^{off}$/h	μ_i/(kcf/MWh)
G1	50	250	100	100	3	3	14.38
G2	10	50	30	30	2	2	14.38
G3	40	80	30	30	3	3	14.38
G4	50	100	40	40	4	4	15.28
G5	100	200	80	80	5	5	14.02

Table A3. Parameters of transmission lines.

Start Node	Termination Node	x_l/(p.u.)	Transmission Restrictions/MW
1	2	0.037	200
1	4	0.016	200
2	3	0.1015	175
2	4	0.117	175
3	6	0.0355	175
4	5	0.037	200
5	6	0.127	200

Table A4. Parameters of gas wells.

Gas Well	$Q_{\omega,\max}$/(kcf/h)	$Q_{\omega,\min}$/(kcf/h)	ρ_ω/(USD/kcf)
GW1	1000	500	5
GW2	1200	600	5.5

Table A5. Parameters of gas storage facility.

$E_{s,\max}^{NG}$/(kcf)	$E_{s,\min}^{NG}$/(kcf)	$Q_{s,\max}^{NG.out}$/(kcf/h)	$Q_{s,\max}^{NG.\text{in}}$/(USD/kcf)	$E_{s,0}^{NG}$/(kcf)	$Q_{\omega.\max}$/(USD/kcf)
2000	200	500	200	1000	1

Table A6. Parameters of natural gas pipelines.

Start Node	Termination Node	C_p/(kcf/Psig)	$M_{p,\max}$	$M_{p,\min}$
1	2	60.6	/	/
2	4	58.1	1.2	1
2	5	47.5	/	/
3	5	58.5	/	/
4	7	58.1	/	/
5	6	69.3	/	/

Table A7. Parameters of natural gas node.

Node	$pr_{n,\max}$/Psig	$pr_{n,\max}$/Psig
1	60	55
2	70	60
3	65	55
4	70	60
5	67	55
6	72	60
7	72	60

References

1. Li, J.; Obara, S. Study on Hydrogen Energy Supply System with Natural Gas Pipeline in China. In Proceedings of the 2019 IEEE PES Asia-Pacific Power and Energy Engineering Conference (APPEEC), Macao, China, 1–4 December 2019; pp. 1–4. [CrossRef]
2. Rohith, P.K.; Priolkar, J.; Kunkolienkar, G.R. Hydrogen: An Innovative and Alternative Energy for the Future. In Proceedings of the 2016 World Conference on Futuristic Trends in Research and Innovation for Social Welfare (Startup Conclave), Coimbatore, India, 29 February–1 March 2016; pp. 1–5. [CrossRef]
3. Zhang, Y.; Zhou, Y.; Song, P.; Liu, W.; Wang, X.; Chen, H.; Lei, X. The Research on Application of Power-to-Heat (P2H) Technologies Combined into Integrated Energy System. In Proceedings of the 2018 International Conference on Power System Technology (POWERCON), Guangzhou, China, 6–8 November 2018; pp. 4537–4543. [CrossRef]
4. Clegg, S.; Mancarella, P. Integrated Modeling and Assessment of the Operational Impact of Power-to-Gas (P2G) on Electrical and Gas Transmission Networks. *IEEE Trans. Sustain. Energy* **2015**, *6*, 1234–1244. [CrossRef]
5. Wu, Q.H.; Qin, Y.J.; Wu, L.L.; Zheng, J.H.; Li, M.S.; Jing, Z.X.; Zhou, X.X.; Wei, F. Optimal operation of integrated energy systems subject to coupled demand constraints of electricity and natural gas. *CSEE J. Power Energy Syst.* **2020**, *6*, 444–457. [CrossRef]

6. Ji, Z.; Kang, C.; Chen, Q.; Xia, Q.; Jiang, C.; Chen, Z.; Xin, J. Low-Carbon Power System Dispatch Incorporating Carbon Capture Power Plants. *IEEE Trans. Power Syst.* **2013**, *28*, 4615–4623. [CrossRef]
7. Li, Y.; Du, Y.; Xiang, K.; Lin, C.; Lin, H.; Yang, Y. Planning Model of Integrated Energy System Considering P2G and Energy Storage. In Proceedings of the 2019 IEEE 3rd Conference on Energy Internet and Energy System Integration (EI2), Changsha, China, 8–10 November 2019; pp. 1246–1251. [CrossRef]
8. Zhang, Y.; Wang, X.; He, J.; Xu, Y.; Pei, W. Optimization of Distributed Integrated Multi-energy System Considering Industrial Process Based on Energy Hub. *J. Mod. Power Syst. Clean Energy* **2020**, *8*, 863–873. [CrossRef]
9. Martínez-Mares, A.; Fuerte-Esquivel, C.R.; de Ingeniería, I. Integrated Energy Flow Analysis in Natural Gas and Electricity Coupled Systems. In Proceedings of the 2011 North American Power Symposium, Boston, MA, USA, 4–6 August 2011; pp. 1–7. [CrossRef]
10. Xie, D.; Kang, L.; Jia, Y.; Chen, H.; Tian, F.; Bai, Y.; Zhang, B.; Cui, X. Low-Carbon Economic Dispatch of Integrated Energy System Considering Hydrogen Mixing in Natural Gas Pipeline. In Proceedings of the 2021 IEEE 5th Conference on Energy Internet and Energy System Integration (EI2), Taiyuan, China, 22–24 October 2021; pp. 160–164. [CrossRef]
11. Tabkhi, F.; Azzaro-Pantel, C.; Pibouleau, L.; Domenech, S. A mathematical framework for modeling and evaluating natural gas pipeline networks under hydrogen injection. *Int. J. Hydrogen Energy* **2008**, *33*, 6222–6231. [CrossRef]
12. Liu, C.; Shahidehpour, M.; Fu, Y.; Li, Z. Security-Constrained Unit Commitment With Natural Gas Transmission Constraints. *IEEE Trans. Power Syst.* **2009**, *24*, 1523–1536. [CrossRef]
13. Li, G.; Zhang, R.; Jiang, T.; Chen, H.; Bai, L.; Li, X. Security-constrained bi-level economic dispatch model for integrated natural gas and electricity systems considering wind power and power-to-gas process. *Appl. Energy* **2017**, *194*, 696–704. [CrossRef]
14. Urbina, M.; Li, Z. A Combined Model for Analyzing the Interdependency of Electrical and Gas Systems. In Proceedings of the 39th North American Power Symposium, Las Cruces, NM, USA, 30 September–2 October 2007.
15. Correa-Posada, C.M.; Sanchez-Martin, P. Gas Network Optimization: A Comparison of Piecewise Linear Models. Available online: http://www.optimization-online.org/DB_HTML/2014/10/4580.html (accessed on 15 February 2022).
16. He, C.; Wu, L.; Liu, T.; Shahidehpour, M. Robust Co-Optimization Scheduling of Electricity and Natural Gas Systems via ADMM. *IEEE Trans. Sustain. Energy* **2017**, *8*, 658–670. [CrossRef]